

Are All Vision Models Created Equal? A Study of the Open-Loop to Closed-Loop Causality Gap

Mathias Lechner^{*1}, Ramin Hasani¹, Alexander Amini¹, Tsun-Hsuan Wang¹,
Thomas Henzinger², and Daniela Rus¹

¹Massachusetts Institute of Technology (MIT)

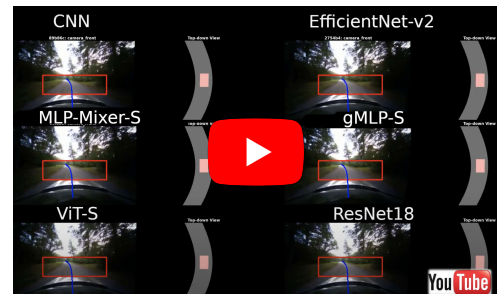
²Institute of Science and Technology Austria (IST Austria)

There is an ever-growing zoo of modern neural network models that can efficiently learn end-to-end control from visual observations. These advanced deep models, ranging from convolutional to patch-based networks, have been extensively tested on offline image classification and regression tasks. In this paper, we study these vision architectures with respect to the open-loop to closed-loop causality gap, i.e., offline training followed by an online closed-loop deployment. This causality gap typically emerges in robotics applications such as autonomous driving, where a network is trained to imitate the control commands of a human. In this setting, two situations arise: 1) Closed-loop testing in-distribution, where the test environment shares properties with those of offline training data. 2) Closed-loop testing under distribution shifts and out-of-distribution. Contrary to recently reported results, we show that *under proper training guidelines*, all vision models perform indistinguishably well on in-distribution deployment, resolving the causality gap. In situation 2, We observe that the causality gap disrupts performance regardless of the choice of the model architecture. Our results imply that the causality gap can be solved in situation one with our proposed training guideline with *any* modern network architecture, whereas achieving out-of-distribution generalization (situation two) requires further investigations, for instance, on data diversity rather than the model architecture.

1. Introduction

The deployment of end-to-end learning systems in robotics applications is increasing due to their ability to efficiently and automatically learn representations from high-dimensional observations such as visual inputs without the need for hand-crafting features, bypassing perception to control.

In this space, a tremendous number of advanced deep learning models have been proposed to perform competitively in end-to-end perception-to-control tasks. For example, patch-based vision architectures such as Vision Transformer (ViT) (Dosovitskiy et al., 2020) have shown to be competitive with models based on convolutional neural networks (CNNs) (Fukushima and Miyake, 1982; Lechner et al., 2022; LeCun et al., 1989) in computer vision applications for which CNNs were the predominant choice. A recent line of research, namely the MLP-Mixer (Tolstikhin et al., 2021), and ConvMixer (Trockman and Kolter, 2022) suggested that the great generalization performance of ViT might be rooted in the patch structure of the inputs rather than the choice of the architecture. There are also works suggesting that self-attention is not crucial in vision Transformers and simply a gating projection in multi-layer perceptrons (MLPs) (Liu et al.,



Video demonstration of vision models in self driving. <https://youtu.be/0GxKzv5Ej88>

^{*}Correspondence E-mail: mlechner@mit.edu

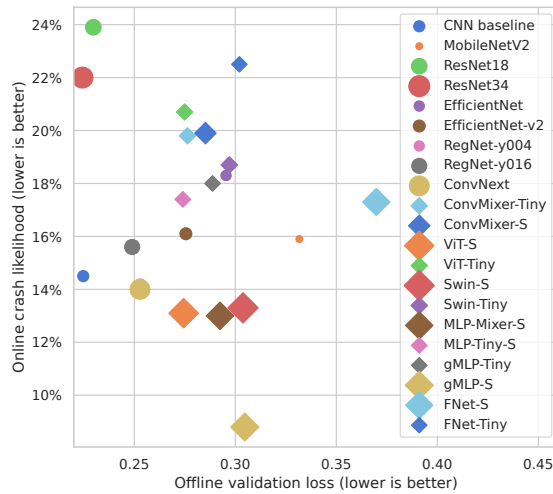


Fig. 1: Online deployment vs. offline training causality gap in perspective. Marker size is linearly proportional to the number of trainable parameters.

2021a) or replacing self-attention sublayer with an unparameterized Fourier Transform (Lee-Thorp et al., 2021) can outperform ViT.

These proposals are largely tested in offline settings where the output decisions of the network do not change the next incoming inputs. In other words, patch-based and mixer models trained offline have not yet been evaluated in a closed-loop with an environment where network actions affect next observations, such as in imitation learning tasks. IL agents typically suffer from a causality gap arising from the transfer of models from open-loop training to closed-loop testing. In this paper, we focus on investigating this gap in a systematic way.

In closed-loop testing, we need to be cognizant of two modes: 1) Closed-loop testing in-distribution. In this setting, we test networks in environments that share similar properties to that of the training environment. 2) Closed-loop testing under distribution shifts and out-of-distribution.

Testing models under both settings requires us to ensure fairness and proper evaluation of the effectiveness of different model architectures in learning robust perception-to-control instances. To this end, we must validate that all baseline models are trained to their best capability given the same amount of hyperparameter optimization budget under a controlled training pipeline.

In an attempt to make a unified evaluation of advanced deep learning models in robot imitation learning tasks, in this paper, we set out to design a series of imitation learning pipelines to train models in a controlled and fair setting and test their generalization capability in and out of distribution.

In particular, we design an end-to-end autonomous driving (AD) IL pipeline based on a photorealistic AD simulation platform called VISTA (Amini et al., 2020), which can test agents in a closed-loop AD environment synthesizing novel views to assess their closed-loop generalization capabilities (Xiao et al., 2021, 2022).

Counterintuitively and in contrast to the recently reported results (Bai et al., 2021; Naseer et al., 2021; Paul and Chen, 2022), we show that no new architecture is needed to bridge the causality gap between offline training and online testing in-distribution, as our controlled training pipeline enables all models to perform remarkably well on the given tasks. Moreover, for achieving out-of-distribution generalization, we observe that the causality gap certainly affects the performance of models, again, almost regardless of the choice of their architecture. These findings suggest the rethinking of the emphasis on the choice of popular models such as Transformers



Fig. 2: Visualization of sample observations used in our end-to-end AD experiment, spanning across various seasons and times of the day.

over CNNs, as other factors such as proper training setup, augmentation strategies, and data diversity play a more important role in generalization in and out of distribution.

To validate our results and make sure our conclusions are not specific to the AD domain, we further extended our experiments (offline training, then online testing) to more standard visual behavior cloning benchmarks such as perception-to-control arcade learning environment (ALE) (Bellemare et al., 2013) tasks. Similar conclusions are then drawn in this case.

Our contributions are summarized below:

1. The design of a unified end-to-end training infrastructure for a fair comparison of advanced deep learning architectures in robot imitation learning applications
2. Studying patch-based architectures and advanced CNNs as agents in closed-loop with their environments via offline training (imitation) and online testing.
3. Discovering new insights about where patch-based architectures generalize better than CNNs and vice versa in test-cases in and out of distribution

2. Background and Related Works

In this section, we first discuss the image processing architectures studied in this work. Moreover, we recapitulate related works on the understanding of how patch-based CV models process information differently than convolutional architectures. Finally, we discuss existing works on bridging the gap between offline training - online generalization.

Patch-based vision architectures. Motivated by the success of Transformers (Vaswani et al., 2017) on natural language processing (NLP) datasets, (Dosovitskiy et al., 2020) introduced the *Vision Transformer* (ViT) by adapting the architecture for computer vision tasks. As transformers operate on a 1-dimensional sequence of vectors, (Dosovitskiy et al., 2020) proposed to convert an image into a sequence by tiling it into patches. Each patch is then flattened into a vector by concatenating all pixel values. Researchers have analyzed the difference between how CNNs and ViTs process images (Raghu et al., 2021). Moreover, it has been claimed that vision transformers are much more robust to image perturbations and occlusions (Naseer et al., 2021), as well as be able to handle distribution-shifts (Bai et al., 2021; Lechner et al., 2021) better than CNNs. However, more recent works have refuted the robustness claims of vision transformers (Fu et al., 2021) by showing that ViTs can be less robust than convolutional networks when considering carefully crafted adversarial attacks.

Swin Transformer (Liu et al., 2021b) modifies the vision transformer by adding a hierarchical structure to the feature sequence of patches. The Swin Transformer applies its attention mechanism not to the full sequence but to a window that is shifted over the entire sequence. By increasing network depth, neighboring windows are merged and pooled into large, less fine-grained windows. This hierarchical processing allows it to use smaller patches without exploding the compute and memory footprint of the model.

MLP-Mixer (Tolstikhin et al., 2021) adapts the idea of vision transformers to map an image to a sequence of patches. This sequence is then processed by alternating plain multi-layer perceptrons (MLP) over the feature and the sequence dimension, i.e., mixing features and mixing spatial information.

gMLP (Liu et al., 2021a) is another MLP-only vision architecture that differs from the MLP-Mixer by introducing multiplicative spatial gating units between the alternating spatial and feature MLPs. Empirical results (Liu et al., 2021a) show that the gMLP has a better accuracy-parameter ratio than the MLP-Mixer.

FNet (Lee-Thorp et al., 2021) replaces the learnable spatial mixing MLP of the MLP-Mixer architecture by a fixed mixing step. In particular, a parameter-free 2-dimensional Fourier transform is applied over the sequence and features dimensions of the input. Although the authors (Lee-Thorp et al., 2021) did not evaluate the model for vision tasks, FNet’s similarity to patch-based MLP architectures makes it a natural candidate for vision tasks.

ConvMixer (Trockman and Kolter, 2022) replace the MLPs of the MLP-mixer architecture by alternating depth-wise and point-wise 1D convolutions. While an MLP mixes all entries of the spatial and feature dimension, the convolutions of the ConvMixer mix only local information, e.g., kernel size was set to 9 in (Trockman and Kolter, 2022). The authors claim a large part of the performance of MLP and vision transformers can be attributed to the patch-based processing instead of the type of mixing representation (Trockman and Kolter, 2022).

Advanced convolutional architectures. Here, we briefly discuss modern variants of CNN architectures.

ResNet (He et al., 2016) add skip connections that bypass the convolutional layers. This simple modification allows training much deeper networks than a pure sequential composition of layers. Consequently, skip connections can be found in any modern neural network architecture, including patch-based and advanced convolutional models.

MobileNetV2 (Sandler et al., 2018) replace the standard convolution operations by depth-wise separable convolutions that process the spatial and channel dimension separately. The resulting network requires fewer floating-point operations to compute, which is beneficial for mobile and embedded applications.

EfficientNet (Tan and Le, 2019) is an efficient convolutional neural network architecture derived from an automated neural architecture search. The objective of the search is to find a network topology that achieves high performance while simultaneously running efficiently on CPU devices.

EfficientNet-v2 fixes the issue of EfficientNets that despite their efficiency on CPU inference, they can be slower than existing architecture types on GPUs at training and inference.

RegNet (Radosavovic et al., 2020) is a neural network family that systematically explores the design space of previously proposed advances in neural network design. The RegNet-Y subfamily specifically scales the width of the network linearly with depth and comprises squeeze-and-excitation blocks.

ConvNext (Liu et al., 2022) is a network that subsumes many recent advances in the design of vision architectures, including better activation functions, replacing batch-norm by layer-normalization, and a larger kernel size into standard ResNets.

Imitation learning (IL). IL describes learning an agent by expert demonstrations consist of observation-action pairs (Schaal, 1999), directly via behavior cloning (Ho and Ermon, 2016), or indirectly via inverse reinforcement learning (Ng and Russell, 2000). When IL agents are deployed online, they most often deviate from the expert demonstrations leading to compounding errors and incorrect inference. Numerous works have tried to address this problem by adding augmentation techniques that collect data from the cloned model in closed-loop settings. This includes methods such as DAGger (Ross and Bagnell, 2010; Ross et al., 2011), state-aware imitation (Desai et al., 2020; Le et al., 2018; Schroecker and Isbell, 2017), pre-trained policies through meta-learning (Duan et al., 2017; Yu et al., 2018), min-max optimization schemes (Baram et al., 2017; Ho and Ermon, 2016; Sun and Ma, 2019; Wu et al., 2019), using insights from causal inference (Janner et al., 2021; Ortega et al., 2021), and using a

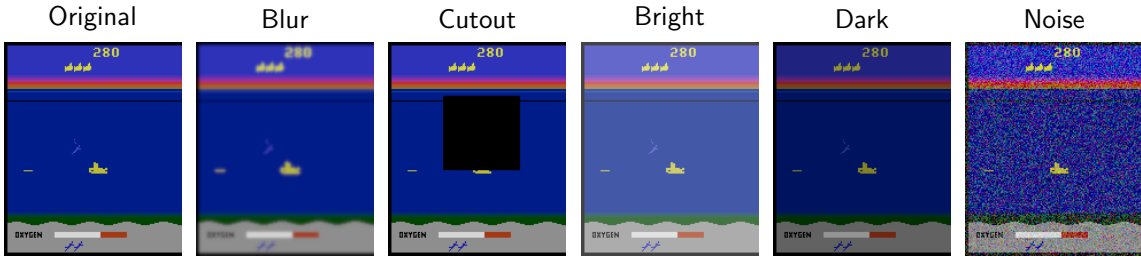


Fig. 3: Visualization of the distribution shifts for the Arcade experiments.

world-model in the loop (Amini et al., 2022; Brunnbauer et al., 2022; Ha and Schmidhuber, 2018; Ullman et al., 2017).

OOD generalization. It is fundamentally challenging for statistical models to tackle OOD problems (Achille and Soatto, 2018; Hendrycks et al., 2021; Liang et al., 2018), such as domain adaptation (Ben-David et al., 2007; Ganin et al., 2016; Gong et al., 2016; Muandet et al., 2013; Tzeng et al., 2017), debiasing (Clark et al., 2019; Geirhos et al., 2018; Huang and Belongie, 2017; Kim et al., 2019; Wang et al., 2018), and even practically more challenging settings where OOD semantics are unlabeled (Arjovsky et al., 2019; Krueger et al., 2021; Rosenfeld et al., 2020; Wang et al., 2021). A large body of recently proposed solutions to OOD generalization, explored causal inference such as causal interventions (Ortega et al., 2021; Wang et al., 2021), designing counterfactual schemes (Niu et al., 2021; Yue et al., 2021), and using attention-based models (Chen et al., 2021; Goyal et al., 2020; Janner et al., 2021; Kim and Canny, 2018; Madan et al., 2020; Yang et al., 2021). Here, our study aims to explore how advanced vision networks compare in terms of OOD generalization in online closed-loop with their environments, when trained offline.

3. Methodology

In this section, we first describe our recipe for how to systematically train end-to-end imitation learning agents offline via a fair hyperparameter tuning pipeline. We then narrate our experimental setup, followed by the method we use for systematic online testing in and out of distribution.

3.1. Fair Training Setup

End-to-end deep learning models are typically benchmarked against each other, where one model showed to be outperforming the other. But is it truly the case? Here, we set out to design a controlled offline training to an online testing setup to fairly investigate how advanced vision baselines compare with each other. The training recipe is as follows:

1. We conduct a systematic hyperparameter tuning process (described in detail in the next subsection) for each of the 21 tested advanced deep models individually. In particular, We ran a grid search over the two most influential hyperparameters, the learning rate and the weight decay rate.
2. We do not perform any early stopping but train a substantial number of optimization steps, which has been shown to be vital for generalization, especially on smaller datasets (Hasani et al., 2021a; Lechner et al., 2020a; Power et al., 2022; Vorbach et al., 2021).

3. We deploy a custom staircase learning rate decay schedule that decreases the learning rate over the training process by dividing the learning rate by four at 60%, 80%, and 93% of the training epochs.
4. We warm up the training by running the first epochs with 1/10th of the initial learning rate in order to have the moments' estimates in Adam (Kingma and Ba, 2014), Batch-Normalization (Ioffe and Szegedy, 2015), and Layer-Normalization (Ba et al., 2016) modules initialized properly.
5. We replace the standard Adam optimizer with AdamW (Loshchilov and Hutter, 2017), which decouples the weight decay rate from the loss function, thus avoiding biasing the moments' estimators of Adam.
6. We apply a rich set of data augmentation techniques, including random brightness, contrast, and saturation modifications, guided policy learning (Levine and Koltun, 2013), and add noise to the expert's actions during exploration (Hasani et al., 2021b).

Baselines We compare all neural network architectures introduced in the related work section. Overall, we test 21 advanced models, including nine modern convolutional networks and 12 modern patch-based architectures. The exact architecture of these models is directly taken from their reported research article. Additionally, we included a controlled vanilla CNN baseline that comprises seven convolutional layers, each followed by a batch-normalization layer and a ReLU activation function. The first convolution applies a 5-by-5 kernel with 64 filters. The following convolution layers all apply a 3-by-3 kernel with 128, 128, 256, 256, 512, and 512 filters, respectively. A global average pooling layer is applied to feature maps of the final convolution layer, followed by a fully-connected layer with 512 units.

3.2. Hyperparameter tuning

In order to have a fair comparison, we perform a systematic hyperparameter tuning process for each architecture. Particularly, we run a grid search over the learning rate and regularization factors (weight decay and dropout rate), which have been shown to have the strongest impact on the performance of the neural networks (Krogh and Hertz, 1991; Loshchilov and Hutter, 2017; Srivastava et al., 2014). The objective function of the tuning process is set to the validation loss of the end-to-end driving task. The grid search first searches for the optimal learning rate by evaluating the network with a learning rate of $\{0.01, 0.003, 0.001, 0.0003\}$. Next, the learning rate is fixed to the best performing one, and the search aims to find the right strength of the regularization factor. We evaluate four levels of regularization strengths measured by a pair (w, d) , where w is the weight decay factor, and d is the dropout rate applied within the network and before the last layer in each architecture. The grid search evaluates the points $\{(10^{-6}, 0), (10^{-5}, 0), (10^{-6}, 0.2), (10^{-4}, 0.2)\}$, i.e., spanning from a low regularization pressure to a strong one.

Figure 4 visualizes the distribution of obtained validation scores of the tested hyperparameters. Most notably, the convolutional architectures tend to have lower variance, i.e., tolerate a wider set of hyperparameters. Moreover, the individual best scores of the models are all in a relatively small range, i.e., between 0.2 and 0.3, demonstrating the necessity of a proper hyperparameter tuning process.

4. Experimental Results

In this section, we describe our findings on a series of end-to-end imitation learning from offline training to online testing tasks, ranging from autonomous driving to many arcade learning environment games.

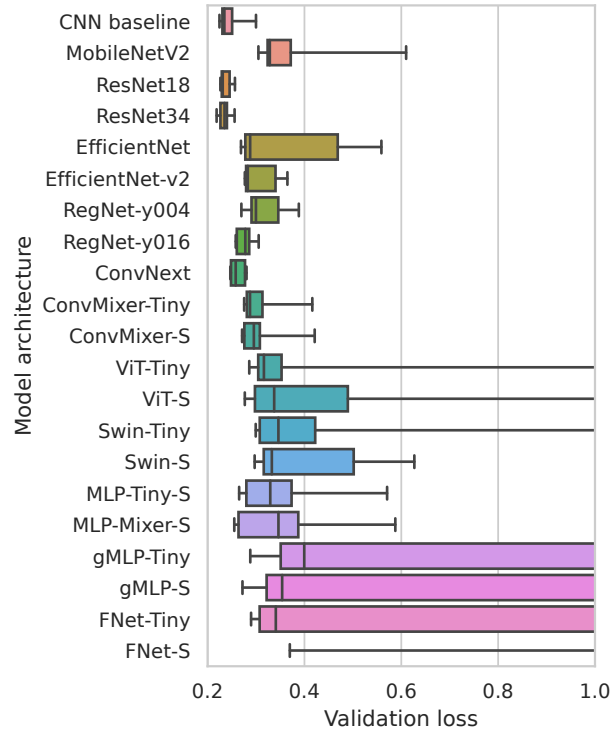


Fig. 4: Box-plot showing the validation loss distribution for the different hyperparameters tested for each model. The whiskers represent the minimum/maximum, the box the 0.25, 0.5, and 0.75 quantiles of the values.

4.1. End-to-end autonomous driving

Our first experiment concerns learning the end-to-end control of an autonomous vehicle. We collect data on a full-scale autonomous vehicle with a 30Hz BFS-PGE-23S3C-CS RGB Camera with resolution 960×600 and 130° . Each image is temporally synchronized with the steering angle estimated by a differential GPS and an IMU to construct a training pair. The dataset consists of roughly 5-hour driving data collected in different times of the day, different road types, and different seasons, e.g., see Figure 2. Among all variations, we use summer and winter data for training set with a fraction put aside for (in-distribution) testing and leave fall, spring, and night data for (out-of-distribution) evaluation. For image preprocessing, we perform center cropping as we focus on lane tracking in this work, and we adopt data augmentation, including randomization in brightness, saturation, hue, and gamma, finally followed by per-image normalization. To improve over compounding error generated by imitation learning, we use Guided Policy Learning (GPL) (Levine and Koltun, 2013) to generate off-orientation training data and teach the policy how to recover from such scenarios (Amini et al., 2022). To test our model in a closed-loop setting, we leverage a high-fidelity data-driven simulator (Amini et al., 2022) that can be built upon the collected dataset. Trained agents are placed within these simulated environments and are capable of perceiving novel viewpoints in the scene as they execute their policies. The resolution of the input images is 48-by-160 pixels, and all models are trained for 600k steps with a batch size of 64.

For each model and data condition pair (summer, winter, fall, spring, and night), we run a total of 200 evaluations. An evaluation consists of the model controlling the vehicle’s steering with a constant velocity until the vehicle either crashes (i.e., leaves the road) or a certain distance has been driven. We report the number of evaluations

Table 1: End-to-end autonomous driving. Numbers show the number of experiment runs that crashed before successful termination. The value in parentheses shows the percentage. The experiments for each model in each column are repeated 200 times. Total number of experiments=21000 (1000 inference experiments for each model in 5 different environments).

Model	Number of crashes						
	Condition: Seen in training:	Summer (in-distribution)	Winter	Fall	Spring	Night	All
CNN baseline		0 (0%)	0 (0%)	13 (7%)	24 (12%)	108 (54%)	145 (15%)
MobileNetV2		0 (0%)	0 (0%)	28 (15%)	48 (24%)	83 (42%)	159 (16%)
ResNet18		0 (0%)	0 (0%)	64 (32%)	57 (29%)	118 (59%)	239 (24%)
ResNet34		0 (0%)	0 (0%)	59 (30%)	46 (23%)	115 (58%)	220 (22%)
EfficientNet		0 (0%)	0 (0%)	33 (17%)	45 (23%)	105 (53%)	183 (19%)
EfficientNet-v2		0 (0%)	0 (0%)	23 (12%)	39 (20%)	99 (50%)	161 (17%)
RegNet-y004		0 (0%)	0 (0%)	18 (9%)	44 (22%)	80 (40%)	142 (15%)
RegNet-y016		0 (0%)	0 (0%)	12 (6%)	48 (24%)	96 (48%)	156 (16%)
ConvNext		0 (0%)	0 (0%)	16 (8%)	49 (25%)	75 (38%)	140 (15%)
ConvMixer-Tiny		0 (0%)	0 (0%)	30 (15%)	58 (29%)	110 (56%)	198 (20%)
ConvMixer-S		0 (0%)	0 (0%)	25 (13%)	63 (32%)	111 (56%)	199 (20%)
ViT-S		0 (0%)	0 (0%)	21 (11%)	40 (20%)	70 (35%)	131 (14%)
ViT-Tiny		0 (0%)	0 (0%)	22 (11%)	67 (34%)	118 (59%)	207 (21%)
Swin-S		0 (0%)	0 (0%)	13 (7%)	55 (28%)	65 (33%)	133 (14%)
Swin-Tiny		0 (0%)	0 (0%)	23 (12%)	65 (33%)	99 (50%)	187 (19%)
MLP-Mixer-S		0 (0%)	0 (0%)	24 (12%)	58 (29%)	48 (24%)	130 (13%)
MLP-Tiny-S		0 (0%)	0 (0%)	1 (1%)	63 (32%)	110 (56%)	174 (18%)
gMLP-Tiny		0 (0%)	0 (0%)	9 (5%)	48 (24%)	123 (62%)	180 (18%)
gMLP-S		0 (0%)	0 (0%)	0 (0%)	57 (29%)	31 (16%)	88 (9%)
FNet-S		0 (0%)	0 (0%)	48 (24%)	71 (36%)	54 (27%)	173 (18%)
FNet-Tiny		0 (0%)	0 (0%)	29 (15%)	63 (32%)	133 (67%)	225 (23%)
Bold threshold				$\leq 5\%$	$\leq 20\%$	$\leq 30\%$	

that terminated with a crash as our performance metric, with an optimal model counting zero crashes.

The result in Table 1 shows the number of crashes for the five different environmental conditions and the aggregated counts over all 1000 evaluation runs. The first two columns show that no crash was observed for any model in the summer and winter conditions. Note that data used for the summer and winter simulation does not overlap with the training data, they only share the season of their data collection process. In the out-of-distribution environment conditions, no model was able to maneuver the vehicle across all 600 runs successfully. The best performing model, the gMLP-S had no crash when simulated in fall, but a significant crash rate of 29% and 16% in the spring and night conditions, respectively. Figure 1 contrasts the offline performance measured by the validation loss on the x-axis with the online performance measured by crash likelihood on the y-axis. When comparing the convolutional neural network with the patch-based architectures, no significant discrepancy is observed.

Table 2: In-distribution online testing of the Arcade Learning Environments. Numbers report the average episode return for 21 models on 13 different games; each model is trained three times and tested 20 times at inference. Total of 16380 experiments. Values within 1/5 of the standard deviation of the best performing model are highlighted in bold.

Model	<i>Alien</i>	<i>Beamrider</i>	<i>Breakout</i>	<i>Defender</i>	<i>Enduro</i>	<i>Frogger</i>	<i>Frostbite</i>	<i>Gopher</i>	<i>Pinball</i>	<i>Pong</i>	<i>Qbert</i>	<i>Seaquest</i>	<i>Spaceinvaders</i>	Ranking
CNN baseline	1388	6541	41	10470	640	544	8026	2088	14239	11	12451	4574	824	3
MobileNetV2	1468	6282	43	8448	576	505	7663	2335	13140	12	12740	4124	784	2
ResNet18	1454	6818	46	10104	642	549	7486	2308	18219	13	12986	4483	750	6
ResNet34	1547	6514	49	11825	610	557	8013	2187	19572	12	12614	4369	766	6
EfficientNet	1408	6406	47	9908	622	560	7490	2328	24018	12	12884	4106	781	5
EfficientNet-v2	1475	6476	46	10168	638	563	8251	2210	19860	12	12785	4275	756	5
RegNet-y004	1499	6630	41	10848	644	547	8128	2194	20970	11	12972	4301	850	4
RegNet-y016	1444	6459	43	10498	663	538	7918	2016	16847	12	12876	4185	839	4
ConvNext	1459	6343	45	11420	591	509	6800	2143	19518	12	12696	4352	769	2
ConvMixer-Tiny	1515	6535	46	9396	636	556	7769	2164	19842	11	12610	4316	798	3
ConvMixer-S	1425	6363	41	9190	625	504	6905	2327	18474	11	12520	4206	769	0
ViT-S	1530	6137	38	9256	583	512	7346	2168	16102	11	12649	4516	813	4
ViT-Tiny	1442	6684	42	8705	603	540	7312	2031	19634	12	12565	4382	841	3
Swin-S	1538	6143	33	9876	518	416	7297	2108	21341	10	13220	4122	791	2
Swin-Tiny	1473	6630	40	9174	595	468	7716	2128	21827	12	12089	4021	843	2
MLP-Mixer-S	1465	6250	38	10058	607	509	7251	2081	18187	11	12111	4301	800	0
MLP-Tiny-S	1542	5874	38	10192	591	513	7443	2009	19518	12	12738	3992	754	2
gMLP-Tiny	1569	6863	38	10589	620	550	7634	1957	17126	-21	13167	4242	783	4
gMLP-S	1451	6520	41	11831	612	544	7562	2058	16642	-21	12584	4159	855	2
FNet-S	1443	6361	41	9645	577	486	7818	2220	17883	13	13132	3873	887	3
FNet-Tiny	1433	6290	38	9570	571	487	7865	2469	20219	11	12951	4474	832	4
Expert policy ± 1/5 std. dev.	1307 ± 67	6979 ± 321	49 ± 3	10495 ± 753	627 ± 18	482 ± 15	7737 ± 358	2222 ± 126	18318 ± 1772	14 ± 1	12995 ± 583	3177 ± 206	699 ± 82	

4.2. Arcade learning environment

As the performance of neural networks is very tasks-specific, a large set of different evaluations are necessary to draw significant conclusions. Here, we study the offline-online generalization gap of vision architectures on a total of 13 different IL tasks. In particular, we use the Arcade Learning Environment (ALE) (Bellemare et al., 2013), which provides a large number of closed-loop environments and images as observations.

The training data for the imitation learning setup are generated by an expert policy in the form of a deep Q-network (DQN) (Mnih et al., 2015) from the stable-baselines3 repository (Raffin et al., 2021). Specifically, we collect the observations and the corresponding suggested action of DQN as labels for the behavior cloning. As regularization, we inject noise into the closed-loop interaction of the data collection process by overwriting 10% of the DQN’s actions with randomly sampled ones. Note that the random actions are only used for driving exploration; the training data contain no random actions.

We collect a total of 2 million data samples for each task, which we split into a training and a validation set with a ratio of 85%:15% of non-overlapping trajectories. We preprocess the observations by converting the images by rescaling them to gray-scale with a resolution of 84-by-84 and stacking the four most recent frames, i.e., a technique known as *deepmind* processor in the literature. For each architecture, we use the tuned hyperparameters from before and train for 200k steps.

Our performance measure is the episodic return, i.e., the non-discounted sum of rewards, when deploying the

Table 3: Mean episode return of the OOD deployment of the Arcade models. Values within 1/5 of the standard deviation of the best performing model are highlighted in bold.

Model	Alien	Beamrider	Qbert	Seaquest	Rank
CNN baseline	877	4889	8137	2906	0
MobileNetV2	922	4723	6360	2218	0
ResNet18	1024	5486	7006	3219	1
ResNet34	990	5167	7140	3465	0
EfficientNet	770	4648	6665	2922	0
EfficientNet-v2	921	4917	7182	3399	0
RegNet-y004	891	5329	7001	3251	1
RegNet-y016	787	4997	5847	2886	0
ConvNext	1292	5443	6970	3505	2
ConvMixer-Tiny	1098	5101	7778	1938	0
ConvMixer-S	1153	5549	8412	2428	2
ViT-S	1025	4353	5983	3177	0
ViT-Tiny	1044	4618	5654	2280	0
Swin-S	1211	5268	8023	2812	1
Swin-Tiny	1188	5203	6512	2670	0
MLP-Mixer-S	1082	4925	6384	3030	0
MLP-Tiny-S	1141	4249	5822	3060	0
gMLP-Tiny	1143	5580	7190	2742	1
gMLP-S	1192	5114	7017	3586	1
FNet-S	1080	5330	9180	3166	2
FNet-Tiny	1043	5318	8479	3262	2

networks in the closed-loop for a total of 20 episodes. We repeat this experiment, including the training process, for three different random seeds. The results are shown in Table 2. For each environment, we highlight scores that are within 1/5 of the standard deviation of the best-performing model in bold. We also rank the different network architectures by counting for how many environments they are bolding threshold. The results show that no single model consistently outperforms other architectures and that overall, each model could achieve an excellent closed-loop performance (with only a few outliers). Nonetheless, we observe a minor trend that conv networks achieve a top (bolded) performance more frequently compared to patch-based networks.

Arcade learning environment under distribution-shift

We also perform an evaluation of how well the models trained on the ALE tasks tolerate a change in the data distribution. In particular, we study the effects of 10 different data modification policies on the closed-loop performance measured in the episodic return of the trained ALE models. The data modification policies are Gaussian blurring with kernel size 3x3 and 5x5, cutting out a 6x6 and 12x12 window in the center of the frame, increasing the brightness by 16 and 32, decreasing the brightness by 16 and 32, and adding uniform noise with a spread of ± 16 and ± 32 (pixel values range from 0 to 255). We select the ALE environments *Alien*, *Beamrider*, *QBert*, and *Seaquest* for our evaluation as most models achieve a decent performance on them, thus avoiding skewing the distribution-shift robustness by a difference in in-distribution performance. Figure 3 visualizes the

different types of applied data modification policies.

The results of the ALE out-of-distribution experiments are shown in Table 3. Contrarily to the in-distribution evaluations, we observe a minor trend of the patch-based models performing slightly better than convolutional neural network architectures in environments with shifted distributions.

5. Conclusion

In this work, we studied the open-loop to closed-loop causality gap where a neural network is trained offline on labeled data but deployed in a closed-loop system where the decisions of the network affect the next observation, i.e., a setting often found in control and robotics. Our study focused on image data and modern vision models, specifically, we compared convolutional neural networks with recently proposed patch-based architectures. Our results showed that if properly trained, any architecture can handle the open-loop to closed-loop causality gap. We also showed a change in the data distribution could have catastrophic consequences on the causality gap.

Our results indicate that more fundamental approaches than advances in vision processing architectures are necessary to handle the causality gap and a possible change in the data distribution simultaneously. A potential future direction could be to look into incorporating discrete (Goyal et al., 2020; Hasani et al., 2019, 2016, 2017) and continuous recurrent mechanisms (Hasani et al., 2020; Lechner and Hasani, 2020; Lechner et al., 2019), and structural state-space models (Gu et al., 2021; Hasani et al., 2022; Lechner et al., 2020b) in the design of our future vision networks.

ACKNOWLEDGMENT

This work was partially supported in parts by the ERC-2020-AdG 101020093. Additionally, it was partially sponsored by the United States Air Force Research Laboratory and the United States Air Force Artificial Intelligence Accelerator and was accomplished under Cooperative Agreement Number FA8750-19-2-1000. The views and conclusions contained in this document are those of the authors and should not be interpreted as representing the official policies, either expressed or implied, of the United States Air Force or the U.S. Government. The U.S. Government is authorized to reproduce and distribute reprints for Government purposes notwithstanding any copyright notation herein. This work was further supported by The Boeing Company and the Office of Naval Research (ONR) Grant N00014-18-1-2830.

References

- A. Achille and S. Soatto. Information dropout: Learning optimal representations through noisy computation. *IEEE transactions on pattern analysis and machine intelligence*, 40(12):2897–2905, 2018.
- A. Amini, I. Gilitschenski, J. Phillips, J. Moseyko, R. Banerjee, S. Karaman, and D. Rus. Learning robust control policies for end-to-end autonomous driving from data-driven simulation. *IEEE Robotics and Automation Letters*, 5(2):1143–1150, 2020.
- A. Amini, T.-H. Wang, I. Gilitschenski, W. Schwarting, Z. Liu, S. Han, S. Karaman, and D. Rus. Vista 2.0: An open, data-driven simulator for multimodal sensing and policy learning for autonomous vehicles. In *2022 International Conference on Robotics and Automation (ICRA)*, pages 2419–2426. IEEE, 2022.

- M. Arjovsky, L. Bottou, I. Gulrajani, and D. Lopez-Paz. Invariant risk minimization. *arXiv preprint arXiv:1907.02893*, 2019.
- J. L. Ba, J. R. Kiros, and G. E. Hinton. Layer normalization. *arXiv preprint arXiv:1607.06450*, 2016.
- Y. Bai, J. Mei, A. L. Yuille, and C. Xie. Are transformers more robust than cnns? *Advances in Neural Information Processing Systems*, 34, 2021.
- N. Baram, O. Ansel, I. Caspi, and S. Mannor. End-to-end differentiable adversarial imitation learning. In *International conference on machine learning (ICML)*, pages 390–399. PMLR, 2017.
- M. G. Bellemare, Y. Naddaf, J. Veness, and M. Bowling. The arcade learning environment: An evaluation platform for general agents. *Journal of Artificial Intelligence Research*, 47:253–279, 2013.
- S. Ben-David, J. Blitzer, K. Crammer, F. Pereira, et al. Analysis of representations for domain adaptation. *Advances in neural information processing systems*, 19:137, 2007.
- A. Brunnbauer, L. Berducci, A. Brandstätter, M. Lechner, R. Hasani, D. Rus, and R. Grosu. Latent imagination facilitates zero-shot transfer in autonomous racing. In *2022 International Conference on Robotics and Automation (ICRA)*, pages 7513–7520. IEEE, 2022.
- L. Chen, K. Lu, A. Rajeswaran, K. Lee, A. Grover, M. Laskin, P. Abbeel, A. Srinivas, and I. Mordatch. Decision transformer: Reinforcement learning via sequence modeling. *arXiv preprint arXiv:2106.01345*, 2021.
- C. Clark, M. Yatskar, and L. Zettlemoyer. Don’t take the easy way out: Ensemble based methods for avoiding known dataset biases. In *Proceedings of the 2019 Conference on Empirical Methods in Natural Language Processing and the 9th International Joint Conference on Natural Language Processing (EMNLP-IJCNLP)*, pages 4069–4082, 2019.
- S. Desai, I. Durugkar, H. Karnan, G. Warnell, J. Hanna, P. Stone, and A. Sony. An imitation from observation approach to transfer learning with dynamics mismatch. *Advances in Neural Information Processing Systems*, 33, 2020.
- A. Dosovitskiy, L. Beyer, A. Kolesnikov, D. Weissenborn, X. Zhai, T. Unterthiner, M. Dehghani, M. Minderer, G. Heigold, S. Gelly, et al. An image is worth 16x16 words: Transformers for image recognition at scale. In *International Conference on Learning Representations (ICLR)*, 2020.
- Y. Duan, M. Andrychowicz, B. C. Stadie, J. Ho, J. Schneider, I. Sutskever, P. Abbeel, and W. Zaremba. One-shot imitation learning. *arXiv preprint arXiv:1703.07326*, 2017.
- Y. Fu, S. Zhang, S. Wu, C. Wan, and Y. Lin. Patch-fool: Are vision transformers always robust against adversarial perturbations? In *International Conference on Learning Representations*, 2021.
- K. Fukushima and S. Miyake. Neocognitron: A self-organizing neural network model for a mechanism of visual pattern recognition. In *Competition and cooperation in neural nets*, pages 267–285. Springer, 1982.
- Y. Ganin, E. Ustinova, H. Ajakan, P. Germain, H. Larochelle, F. Laviolette, M. Marchand, and V. Lempitsky. Domain-adversarial training of neural networks. *The journal of machine learning research*, 17(1):2096–2030, 2016.

- R. Geirhos, P. Rubisch, C. Michaelis, M. Bethge, F. A. Wichmann, and W. Brendel. Imagenet-trained cnns are biased towards texture; increasing shape bias improves accuracy and robustness. In *International Conference on Learning Representations (ICLR)*, 2018.
- M. Gong, K. Zhang, T. Liu, D. Tao, C. Glymour, and B. Schölkopf. Domain adaptation with conditional transferable components. In *International conference on machine learning (ICML)*, pages 2839–2848. PMLR, 2016.
- A. Goyal, A. Lamb, J. Hoffmann, S. Sodhani, S. Levine, Y. Bengio, and B. Schölkopf. Recurrent independent mechanisms. In *International Conference on Learning Representations*, 2020.
- A. Gu, K. Goel, and C. Re. Efficiently modeling long sequences with structured state spaces. In *International Conference on Learning Representations*, 2021.
- D. Ha and J. Schmidhuber. World models. *arXiv preprint arXiv:1803.10122*, 2018.
- R. Hasani, A. Amini, M. Lechner, F. Naser, R. Grosu, and D. Rus. Response characterization for auditing cell dynamics in long short-term memory networks. In *2019 International Joint Conference on Neural Networks (IJCNN)*, pages 1–8. IEEE, 2019.
- R. Hasani, M. Lechner, A. Amini, D. Rus, and R. Grosu. The natural lottery ticket winner: Reinforcement learning with ordinary neural circuits. In *Proceedings of the 2020 International Conference on Machine Learning*. JMLR. org, 2020.
- R. Hasani, M. Lechner, A. Amini, L. Liebenwein, M. Tschaikowski, G. Teschl, and D. Rus. Closed-form continuous-depth models. *arXiv preprint arXiv:2106.13898*, 2021a.
- R. Hasani, M. Lechner, A. Amini, D. Rus, and R. Grosu. Liquid time-constant networks. *Proceedings of the AAAI Conference on Artificial Intelligence*, 35(9):7657–7666, May 2021b.
- R. Hasani, M. Lechner, T.-H. Wang, M. Chahine, A. Amini, and D. Rus. Liquid structural state-space models. *arXiv preprint arXiv:2209.12951*, 2022.
- R. M. Hasani, D. Haerle, and R. Grosu. Efficient modeling of complex analog integrated circuits using neural networks. In *2016 12th Conference on Ph. D. Research in Microelectronics and Electronics (PRIME)*, pages 1–4. IEEE, 2016.
- R. M. Hasani, D. Haerle, C. F. Baumgartner, A. R. Lomuscio, and R. Grosu. Compositional neural-network modeling of complex analog circuits. In *2017 International Joint Conference on Neural Networks (IJCNN)*, pages 2235–2242. IEEE, 2017.
- K. He, X. Zhang, S. Ren, and J. Sun. Deep residual learning for image recognition. In *Proceedings of the IEEE conference on computer vision and pattern recognition*, pages 770–778, 2016.
- D. Hendrycks, K. Zhao, S. Basart, J. Steinhardt, and D. Song. Natural adversarial examples. In *Proceedings of the IEEE/CVF Conference on Computer Vision and Pattern Recognition (CVPR)*, pages 15262–15271, 2021.
- J. Ho and S. Ermon. Generative adversarial imitation learning. *arXiv preprint arXiv:1606.03476*, 2016.
- X. Huang and S. Belongie. Arbitrary style transfer in real-time with adaptive instance normalization. In *Proceedings of the IEEE International Conference on Computer Vision (ICCV)*, pages 1501–1510, 2017.

- S. Ioffe and C. Szegedy. Batch normalization: Accelerating deep network training by reducing internal covariate shift. In *International conference on machine learning*, pages 448–456. PMLR, 2015.
- M. Janner, Q. Li, and S. Levine. Reinforcement learning as one big sequence modeling problem. *arXiv preprint arXiv:2106.02039*, 2021.
- B. Kim, H. Kim, K. Kim, S. Kim, and J. Kim. Learning not to learn: Training deep neural networks with biased data. In *Proceedings of the IEEE/CVF Conference on Computer Vision and Pattern Recognition (CVPR)*, pages 9012–9020, 2019.
- J. Kim and J. Canny. Explainable deep driving by visualizing causal attention. In *Explainable and Interpretable Models in Computer Vision and Machine Learning*, pages 173–193. Springer, 2018.
- D. P. Kingma and J. Ba. Adam: A method for stochastic optimization. *arXiv preprint arXiv:1412.6980*, 2014.
- A. Krogh and J. Hertz. A simple weight decay can improve generalization. *Advances in neural information processing systems*, 4, 1991.
- D. Krueger, E. Caballero, J.-H. Jacobsen, A. Zhang, J. Binas, D. Zhang, R. Le Priol, and A. Courville. Out-of-distribution generalization via risk extrapolation (rex). In *International conference on machine learning (ICML)*, pages 5815–5826. PMLR, 2021.
- H. Le, N. Jiang, A. Agarwal, M. Dudík, Y. Yue, and H. Daumé. Hierarchical imitation and reinforcement learning. In *International conference on machine learning (ICML)*, pages 2917–2926. PMLR, 2018.
- M. Lechner and R. Hasani. Learning long-term dependencies in irregularly-sampled time series. *arXiv preprint arXiv:2006.04418*, 2020.
- M. Lechner, R. Hasani, M. Zimmer, T. A. Henzinger, and R. Grosu. Designing worm-inspired neural networks for interpretable robotic control. In *International Conference on Robotics and Automation (ICRA)*, pages 87–94, 2019.
- M. Lechner, R. Hasani, A. Amini, T. A. Henzinger, D. Rus, and R. Grosu. Neural circuit policies enabling auditable autonomy. *Nature Machine Intelligence*, 2(10):642–652, 2020a.
- M. Lechner, R. Hasani, D. Rus, and R. Grosu. Gershgorin loss stabilizes the recurrent neural network compartment of an end-to-end robot learning scheme. In *2020 IEEE International Conference on Robotics and Automation (ICRA)*, pages 5446–5452. IEEE, 2020b.
- M. Lechner, R. Hasani, R. Grosu, D. Rus, and T. A. Henzinger. Adversarial training is not ready for robot learning. In *2021 IEEE International Conference on Robotics and Automation (ICRA)*, pages 4140–4147. IEEE, 2021.
- M. Lechner, R. Hasani, Z. Babaiee, R. Grosu, D. Rus, T. A. Henzinger, and S. Hochreiter. Entangled residual mappings. *arXiv preprint arXiv:2206.01261*, 2022.
- Y. LeCun, B. Boser, J. S. Denker, D. Henderson, R. E. Howard, W. Hubbard, and L. D. Jackel. Backpropagation applied to handwritten zip code recognition. *Neural computation*, 1(4):541–551, 1989.
- J. Lee-Thorp, J. Ainslie, I. Eckstein, and S. Ontanon. Fnet: Mixing tokens with fourier transforms. *arXiv preprint arXiv:2105.03824*, 2021.

- S. Levine and V. Koltun. Guided policy search. In *International conference on machine learning (ICML)*, pages 1–9. PMLR, 2013.
- S. Liang, Y. Li, and R. Srikant. Enhancing the reliability of out-of-distribution image detection in neural networks. In *International Conference on Learning Representations (ICLR)*, 2018.
- H. Liu, Z. Dai, D. R. So, and Q. V. Le. Pay attention to mlps. *arXiv preprint arXiv:2105.08050*, 2021a.
- Z. Liu, Y. Lin, Y. Cao, H. Hu, Y. Wei, Z. Zhang, S. Lin, and B. Guo. Swin transformer: Hierarchical vision transformer using shifted windows. *arXiv preprint arXiv:2103.14030*, 2021b.
- Z. Liu, H. Mao, C.-Y. Wu, C. Feichtenhofer, T. Darrell, and S. Xie. A convnet for the 2020s. In *Proceedings of the IEEE/CVF Conference on Computer Vision and Pattern Recognition*, pages 11976–11986, 2022.
- I. Loshchilov and F. Hutter. Decoupled weight decay regularization. *arXiv preprint arXiv:1711.05101*, 2017.
- K. Madan, N. R. Ke, A. Goyal, B. Schölkopf, and Y. Bengio. Fast and slow learning of recurrent independent mechanisms. In *International Conference on Learning Representations (ICLR)*, 2020.
- V. Mnih, K. Kavukcuoglu, D. Silver, A. A. Rusu, J. Veness, M. G. Bellemare, A. Graves, M. Riedmiller, A. K. Fidjeland, G. Ostrovski, et al. Human-level control through deep reinforcement learning. *nature*, 518(7540): 529–533, 2015.
- K. Muandet, D. Balduzzi, and B. Schölkopf. Domain generalization via invariant feature representation. In *International conference on machine learning (ICML)*, pages 10–18. PMLR, 2013.
- M. M. Naseer, K. Ranasinghe, S. H. Khan, M. Hayat, F. Shahbaz Khan, and M.-H. Yang. Intriguing properties of vision transformers. *Advances in Neural Information Processing Systems*, 34, 2021.
- A. Y. Ng and S. Russell. Algorithms for inverse reinforcement learning. In *in Proc. 17th International Conf. on Machine Learning*. Citeseer, 2000.
- Y. Niu, K. Tang, H. Zhang, Z. Lu, X.-S. Hua, and J.-R. Wen. Counterfactual vqa: A cause-effect look at language bias. In *Proceedings of the IEEE/CVF Conference on Computer Vision and Pattern Recognition (CVPR)*, pages 12700–12710, 2021.
- P. A. Ortega, M. Kunesch, G. Delétang, T. Genewein, J. Grau-Moya, J. Veness, J. Buchli, J. Degraeve, B. Piot, J. Perolat, et al. Shaking the foundations: delusions in sequence models for interaction and control. *arXiv preprint arXiv:2110.10819*, 2021.
- S. Paul and P.-Y. Chen. Vision transformers are robust learners. In *Proceedings of the AAAI Conference on Artificial Intelligence*, volume 36, pages 2071–2081, 2022.
- A. Power, Y. Burda, H. Edwards, I. Babuschkin, and V. Misra. Grokking: Generalization beyond overfitting on small algorithmic datasets. *arXiv preprint arXiv:2201.02177*, 2022.
- I. Radosavovic, R. P. Kosaraju, R. Girshick, K. He, and P. Dollár. Designing network design spaces. In *Proceedings of the IEEE/CVF conference on computer vision and pattern recognition*, pages 10428–10436, 2020.

- A. Raffin, A. Hill, A. Gleave, A. Kanervisto, M. Ernestus, and N. Dormann. Stable-baselines3: Reliable reinforcement learning implementations. *Journal of Machine Learning Research*, 22(268):1–8, 2021. URL <http://jmlr.org/papers/v22/20-1364.html>.
- M. Raghu, T. Unterthiner, S. Kornblith, C. Zhang, and A. Dosovitskiy. Do vision transformers see like convolutional neural networks? *Advances in Neural Information Processing Systems*, 34, 2021.
- E. Rosenfeld, P. K. Ravikumar, and A. Risteski. The risks of invariant risk minimization. In *International Conference on Learning Representations (ICLR)*, 2020.
- S. Ross and D. Bagnell. Efficient reductions for imitation learning. In *Proceedings of the thirteenth international conference on artificial intelligence and statistics*, pages 661–668. JMLR Workshop and Conference Proceedings, 2010.
- S. Ross, G. Gordon, and D. Bagnell. A reduction of imitation learning and structured prediction to no-regret online learning. In *Proceedings of the fourteenth international conference on artificial intelligence and statistics*, pages 627–635. JMLR Workshop and Conference Proceedings, 2011.
- M. Sandler, A. Howard, M. Zhu, A. Zhmoginov, and L.-C. Chen. Mobilenetv2: Inverted residuals and linear bottlenecks. In *Proceedings of the IEEE conference on computer vision and pattern recognition*, pages 4510–4520, 2018.
- S. Schaal. Is imitation learning the route to humanoid robots? *Trends in cognitive sciences*, 3(6):233–242, 1999.
- Y. Schroecker and C. Isbell. State aware imitation learning. In *Proceedings of the 31st International Conference on Neural Information Processing Systems*, pages 2915–2924, 2017.
- N. Srivastava, G. Hinton, A. Krizhevsky, I. Sutskever, and R. Salakhutdinov. Dropout: a simple way to prevent neural networks from overfitting. *The journal of machine learning research*, 15(1):1929–1958, 2014.
- M. Sun and X. Ma. Adversarial imitation learning from incomplete demonstrations. *arXiv preprint arXiv:1905.12310*, 2019.
- M. Tan and Q. Le. Efficientnet: Rethinking model scaling for convolutional neural networks. In *International conference on machine learning*, pages 6105–6114. PMLR, 2019.
- I. Tolstikhin, N. Houlsby, A. Kolesnikov, L. Beyer, X. Zhai, T. Unterthiner, J. Yung, A. Steiner, D. Keysers, J. Uszkoreit, et al. Mlp-mixer: An all-mlp architecture for vision. *arXiv preprint arXiv:2105.01601*, 2021.
- A. Trockman and J. Z. Kolter. Patches are all you need? *arXiv preprint arXiv:2201.09792*, 2022.
- E. Tzeng, J. Hoffman, K. Saenko, and T. Darrell. Adversarial discriminative domain adaptation. In *Proceedings of the IEEE conference on Computer Vision and Pattern Recognition (CVPR)*, pages 7167–7176, 2017.
- T. D. Ullman, E. Spelke, P. Battaglia, and J. B. Tenenbaum. Mind games: Game engines as an architecture for intuitive physics. *Trends in cognitive sciences*, 21(9):649–665, 2017.
- A. Vaswani, N. Shazeer, N. Parmar, J. Uszkoreit, L. Jones, A. N. Gomez, Ł. Kaiser, and I. Polosukhin. Attention is all you need. In *Advances in neural information processing systems*, pages 5998–6008, 2017.
- C. Vorbach, R. Hasani, A. Amini, M. Lechner, and D. Rus. Causal navigation by continuous-time neural networks. *arXiv preprint arXiv:2106.08314*, 2021.

- H. Wang, Z. He, Z. C. Lipton, and E. P. Xing. Learning robust representations by projecting superficial statistics out. In *International Conference on Learning Representations (ICLR)*, 2018.
- T. Wang, C. Zhou, Q. Sun, and H. Zhang. Causal attention for unbiased visual recognition. In *Proceedings of the IEEE/CVF International Conference on Computer Vision (ICCV)*, pages 3091–3100, 2021.
- Y.-H. Wu, N. Charoenphakdee, H. Bao, V. Tangkaratt, and M. Sugiyama. Imitation learning from imperfect demonstration. In *International conference on machine learning (ICML)*, pages 6818–6827. PMLR, 2019.
- W. Xiao, R. Hasani, X. Li, and D. Rus. Barriernet: A safety-guaranteed layer for neural networks. *arXiv preprint arXiv:2111.11277*, 2021.
- W. Xiao, T.-H. Wang, M. Chahine, A. Amini, R. Hasani, and D. Rus. Differentiable control barrier functions for vision-based end-to-end autonomous driving. *arXiv preprint arXiv:2203.02401*, 2022.
- X. Yang, H. Zhang, G. Qi, and J. Cai. Causal attention for vision-language tasks. In *Proceedings of the IEEE/CVF Conference on Computer Vision and Pattern Recognition (CVPR)*, pages 9847–9857, 2021.
- T. Yu, P. Abbeel, S. Levine, and C. Finn. One-shot hierarchical imitation learning of compound visuomotor tasks. *arXiv preprint arXiv:1810.11043*, 2018.
- Z. Yue, T. Wang, Q. Sun, X.-S. Hua, and H. Zhang. Counterfactual zero-shot and open-set visual recognition. In *Proceedings of the IEEE/CVF Conference on Computer Vision and Pattern Recognition (CVPR)*, pages 15404–15414, 2021.